The transcriptome of the mosquito host *Anopheles gambiae* upon infection by different selected lines of the microsporidian parasite *Vavraia culicis*

Luís M. Silva [1,2] *

[1] Institute of Biology, University of Neuchâtel, Rue Emilie-Argand 11, 2000 Neuchâtel, Switzerland

[2] Department of Zoology, University of British Columbia, 6270 University Boulevard, Vancouver, BC V6T 1Z4, Canada

* Corresponding author: luis.silva@ubc.ca

ORCID

LMS: 0000-0002-8203-4006

Abstract (204)

Understanding host-parasite interactions is of the utmost importance for disease prediction, prevention and management. Hence, this study assessed the transcriptional response of the primary malaria vector, *Anopheles gambiae*, to infection with several lines of the candidate vector-control parasite, the microsporidian *Vavraia culicis*. These parasite lines were selected for early or late transmission within this host. Previous studies extensively described them phenotypically, differing in their virulence, infection dynamics and host exploitation. Using RNA sequencing, gene expression profiles were analyzed in *An. gambiae* mosquitoes infected with early-transmission-selected, late-transmission-selected, and unselected (*Stock*) *V. culicis* lines, as well as in uninfected controls. The results revealed distinct transcriptional changes associated with each parasite line. Early-selected parasites induced a broader immune response than late-selected ones. Differential expression of immune-related genes, including *Toll-interacting protein* and *Protein ERGIC-53,* was identified. Additionally, significant changes were observed in pathways related to Golgi membrane function and oxidative stress response, particularly in response to early-selected parasites. These findings highlight the evolutionary pressures shaping host-parasite coevolution and provide insight into how parasite transmission traits can influence the mosquito's immune response and regulation. This work provides a foundation for future studies on mosquito-microsporidia dynamics and potential applications for vector control strategies, particularly in the context of *Plasmodium* control.

Background (1192)

Mosquitoes encounter numerous parasites throughout their life cycle [1–6]. Among them, one fungal phylum has drawn significant attention from vector biologists due to its potential as a biological control agent against vector-borne diseases [7–9]. This group, Microsporidia, consists of unicellular intracellular parasites that infect a wide range of organisms, from honeybees to humans, and span diverse ecological niches, including soil and aquatic environments [7, 10–14].

Microsporidian species that infect mosquitoes are predominantly aquatic, as they are adapted to target mosquito larvae that also live and feed in water bodies. The most extensively studied species in this group is *Vavraia culicis* (Order: Glugeida, Family: Pleistophoridae). Like other mosquito-infecting microsporidia, *V. culicis* reaches the gut after ingestion, infecting the host gut cells along the extracellular matrix [15]. A key feature of microsporidian spores facilitates this process: the polar tube. This harpoon-like, protein-based apparatus, typically coiled within the spore, enables the parasite to inject the sporoplasm (containing all genetic material) directly into the host cell and start parasite replication. Once the infected cell reaches its maximum capacity of spores, it lyses, releasing the newly formed spores. In *V. culicis*, this cycle repeats multiple times in the gut, followed by the fat body. These

spores will get transmitted into a new host through one of two ways: horizontal transmission, in adult mosquitoes that die on water, release the spores, which infect nearby larvae and restart the infection cycle; Transovum (vertical) transmission, where the laid eggs are covered in spores and infect other larvae either through cannibalism or contamination of the water body [15].

In a time when strategies to control the public health toll of vector-borne diseases are starting to fall short in efficiency, microsporidian parasites offer a possible solution [7, 8, 16, 17], particularly *V. culicis* with its ease of culture in the lab [18–21], [18–21]and potentially Microsporidia MB [8, 22][8, 22]. Several studies have demonstrated that co-infection with *V. culicis* impairs the growth of *Plasmodium spp.* (i.e., malaria-causing parasite) development within its mosquito vectors, *Anopheles spp.*, and the same has been hypothesized for vector-borne diseases transmitted by *Aedes aegypti* (e.g., dengue) [23]. Additionally, *V. culicis* has been shown to enhance the efficacy of insecticides against mosquitoes by restoring their sensitivity to these chemicals [16]. Since *V. culicis* is not cleared by *Anopheles* mosquitoes [24], it maintains its prevalence in mosquito populations. Although a lot has been done to understand infection by *V. culicis* in *Anopheles* mosquitoes [20, 24–29], research has fallen short in describing the molecular mechanisms and pathways involved in the infection and response to this parasite, let alone the underpinnings of its *Plasmodium*-inhibitory effect.

When considering mosquito infections with *Plasmodium spp.,* it is essential to acknowledge that this parasite can only be transmitted by mosquitoes that live long enough for the parasite to develop (e.g., approximately 20 days for *Plasmodium berghei*). Hence, this setting may also select for co-infecting parasites that can survive for such a long time within the host. In the case of *V. culicis,* a short or a long time within the host might affect its *Plasmodium*-inhibitory potential. Moreover, despite its small genome [14, 28, 30], which could hinder the number of genes where mutations can occur, *V. culicis* has been shown to evolve rapidly [25]. Taking this into consideration, Silva and Koella (2024) artificially selected *V. culicis* that: i) killed the host *Anopheles gambiae* (Order: Diptera, Family: Culicidae) faster and therefore spent less time within it (host death and release of spores approximately at 1 to 7 days of adulthood, hereafter *Early* regime); or ii) allowed the host to live longer and therefore remained in its system for longer too (host death and release of spores approximately at 20 to 30 days of adulthood, hereafter *Late* regime). Surprisingly, they found more time within the host selected the parasite lines of *V. culicis* to be more virulent (i.e., mosquitoes infected with *Late* parasites had a mean time to death of 15.31 ± 0.22 days; *Early* 18.17 ± 0.01; and *Stock* 20.31 ± 0.56), faster parasite development, and higher spore burdens (for day 10 of adulthood: *Late* with 239,500 ± 23,352; *Early* with 98,080 ± 14,853; and *Stock* with 78,900 ± 11,919 spores per mosquito) throughout their life (which will reflect in higher transmission rates upon death), when compared to lines selected to spend less time within their host, or the unselected stock laboratory population of the parasite (hereafter referred to as *Stock*) [25]. These findings reinforce the potential of this microsporidian species as a biological control agent, as higher replication of *V. culicis* in long-lived mosquitoes might increase its *Plasmodium*-inhibitory effect. The

potential increase in the inhibitory effect is due to two main hypotheses for how the inhibitory process takes place: resource competition and collateral immune response, both of which are parasite growth-dependent.

Thus, in this study, I aimed to characterize the response of the host *An. gambiae* to infection with unselected and selected lines of *V. culicis* using RNA sequencing (RNA-seq). With this approach, I had two main aims: i) describe the host response to the unselected *Stock* population of *V. culicis*; and ii) compare the host response to five *Early* from five *Late* selected lines of *V. culicis* obtained from Silva and Koella (2024) (Fig. 1). Through the inclusion of these selected lines, variability in parasite treatments was increased, which may provide insights into which expression patterns are more readily available or likely to evolve in response to different parasite challenges. An uninfected mosquito treatment (hereafter *Uninfected)* was also included as a baseline for the *Stock*-infected mosquito treatment. The time-point selected to assess their transcriptome was day 10 of adulthood for two reasons: i) previous results have shown all infected mosquitoes, regardless of the parasite treatment, are actively releasing infective spores in high numbers, and therefore most likely to induce a host response that can be detected; ii) an assessment of the host response during the early stages of infection is more likely to show clear differences between the parasites, which would be more informative. When considering host immunity, mosquitoes do not possess an adaptive immune system. Instead, their immune defences are mediated by innate immunity, with critical pathways, such as the Toll, Imd, and JAK-STAT pathways, involved in parasite recognition and elimination [31, 32].

The findings of this study provide the first insights into the *An. gambiae* transcriptional response to infection by *V. culicis*, while also demonstrating how parasite evolution drives changes in genome expression, thereby impacting the mosquito's ability to respond to infection. Such insights have been gained in *Ae. aegypti,* a vector of dengue, unveiling a weak immune response but significant up-regulation in lectins and CLIP-domain serine proteases [33], both effectors involved in innate immunity and its signalling [34]. This study complements previous work on these *V. culicis* lines, providing a more comprehensive understanding of this host-parasite interaction. Moreover, the data presented here have important implications for a more general understanding of parasite fitness, as well as mosquito vector competence for vector-borne parasites. Understanding the molecular basis of interactions is crucial for designing effective vector control strategies that exploit the natural evolutionary pressures acting on mosquito-parasite systems [35].

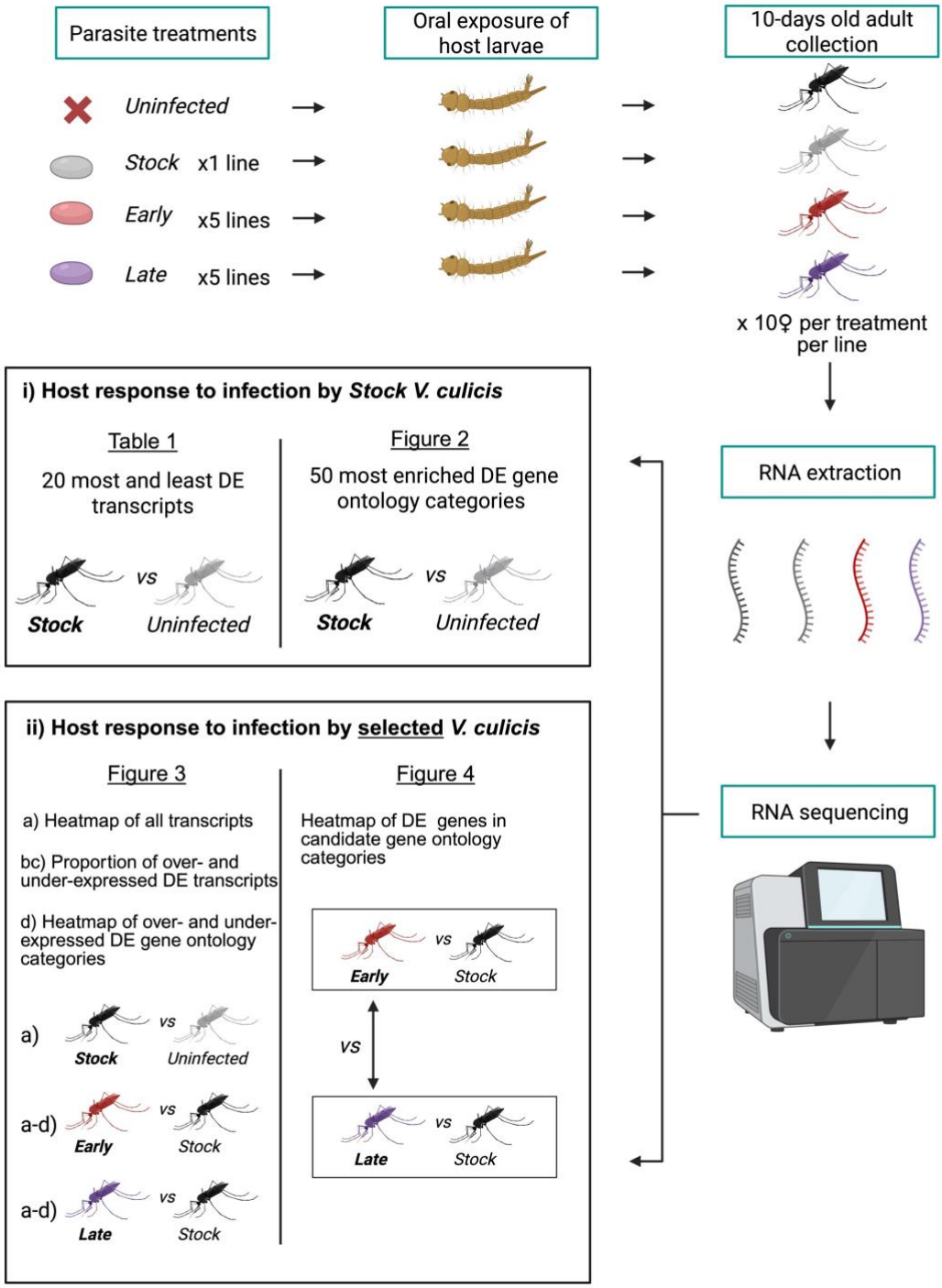

Figure 1. Illustration of the experimental workflow and results. *Anopheles gambiae* mosquito larvae were either uninfected or infected with one of three different sets of lines of the parasite *Vavraia culicis,* to create the following four experimental groups: (1) uninfected mosquitoes (*Uninfected*); (2) mosquitoes infected with spores from an unselected *V. culicis* line (*Stock*); (3) mosquitoes infected with spores from a *V. culicis* line previously selected for early transmission from mosquito hosts (*Early*); and (4) mosquitoes infected with spores from a *V. culicis* line previously selected for late transmission from mosquito hosts (*Late*). After larval infection and subsequent pupation, adult mosquitoes were

collected at day 10 post-adult emergence and pooled to create 10 individuals per biological replicate for RNA extraction (10 females × 5 biological replicates). Then, differences in host response to the presence/absence of the parasite were assessed. First, the 20 most and least expressed transcripts in *Stock*-infected mosquitoes, comparatively to *Uninfected* (Table 1), were identified, as well as the most represented gene ontology (GO) categories and the proportion of genes DE (Fig. 2). Second, all DE transcripts were presented according to their respective (GO) biological process. The latter was followed by a heatmap of the GO categories that are upregulated/downregulated in infection by the *Early* and *Late* parasites, compared to the *Stock* parasite (Fig. 3). Third, selected candidate GO categories from Figure 3 that differed the most between *Early* and *Late* were compared. The expression of the transcripts from these categories was then tested for differences between selection regimes (Fig. 4).

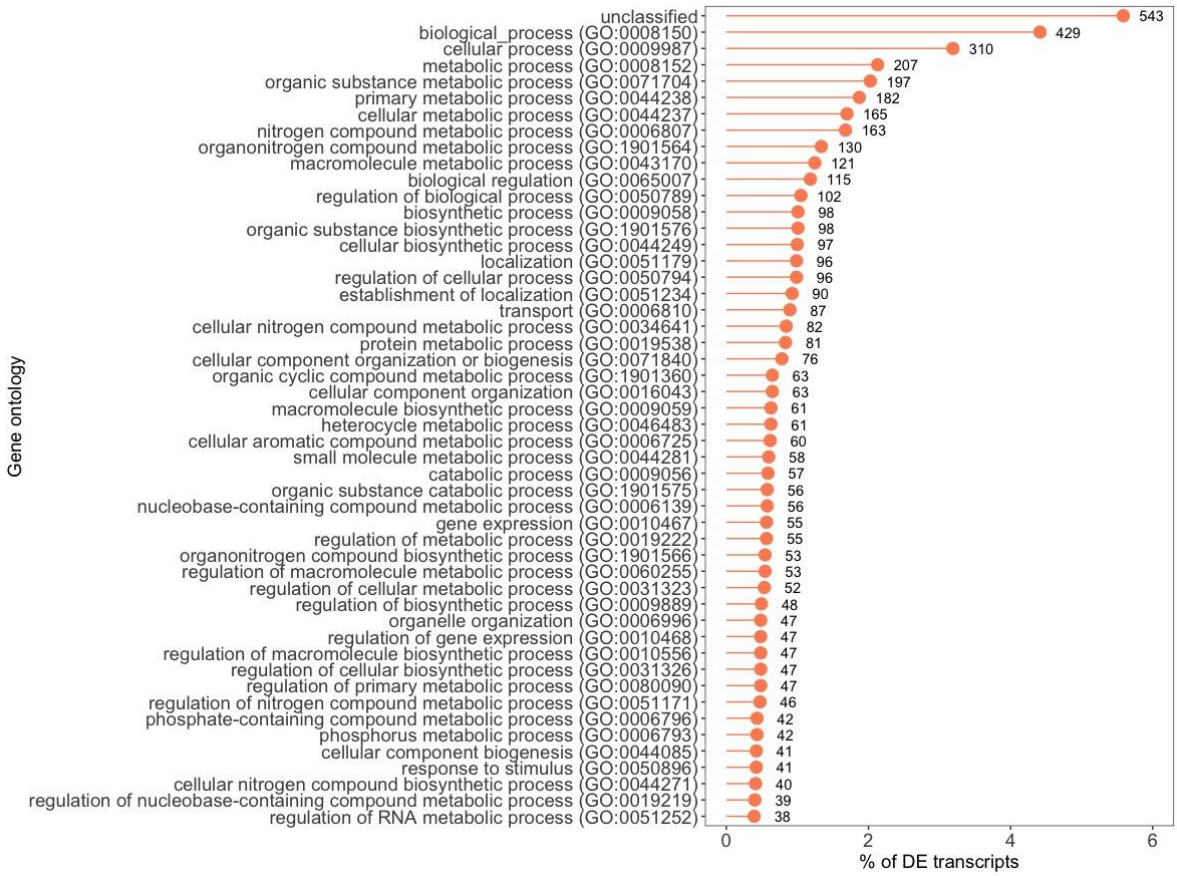

Figure 2. The most enriched gene ontology categories in infected mosquitoes compared to uninfected mosquitoes. Percentage of differentially expressed (DE) transcripts in *An. gambiae* infected with *Stock V. culicis,* compared to *Uninfected* hosts. The plot shows the 50 most enriched gene ontology categories, the percentage of DE transcripts per category, and the absolute number of transcripts (on the right of each dot).

Table 1. Most up-and down-regulated genes in mosquitoes upon infection with the *Stock V. culicis* parasite compared to *Uninfected*. The host transcriptomic profile of an unselected *Stock V. culicis* parasite during infection was compared to that of the uninfected host. The 20 transcripts with the highest and lowest expression, compared to the control, are presented. Fold change and *p*-value were calculated using the transcriptional expression of four technical replicates per treatment (where the same pooled sample (i.e., a single biological replicate) is measured four times). See materials and methods for more details. The *p*-value was adjusted using the Benjamini-Hochberg correction method for each comparison, controlling for a false discovery rate ($p < 0.05$).

#	Gene ID	Gene name	Fold change	Adj. *p*
1	LOC3291958	Putative uncharacterized protein DDB_G0271606	-1680.95	< 0.001
2	LOC133393242	Uncharacterized	-306.13	< 0.001
3	LOC1281554	Protein CIMAP1D	-250.60	< 0.001
4	LOC1271479	Uncharacterized	-246.11	< 0.001
5	LOC133393316	Uncharacterized	-195.71	< 0.001
6	LOC1281083	Arginine kinase 1	-191.24	< 0.001
7	LOC1273786	Serine/arginine-rich splicing factor 2	-190.72	< 0.001
8	LOC133394019	Nucleosome assembly protein 1-like 1	-164.62	< 0.001
9	LOC133391046	Putative cyclin-dependent serine/threonine-protein kinase DDB_G0272797/DDB_G0274007	-161.63	< 0.001
10	LOC1271272	Uncharacterized	-149.47	< 0.001
11	LOC5667228	Uncharacterized	-133.19	< 0.001
12	LOC1269550	Uncharacterized	-126.11	< 0.001
13	LOC1270351	Uncharacterized	-123.92	< 0.001
14	LOC133391930	Uncharacterized	-121.19	< 0.001
15	LOC1277465	Uncharacterized	-119.77	< 0.001
16	LOC133391419	Uncharacterized	-107.89	< 0.001
17	LOC11175695	Uncharacterized	-107.77	< 0.001
18	LOC1278052	Cytosol aminopeptidase	-103.75	< 0.001
19	LOC1267823	Uncharacterized	-95.91	< 0.001
20	LOC4576455	Dynein regulatory complex subunit 4	-89.14	< 0.001
1	LOC1281665	Uncharacterized	13.30	< 0.001
2	LOC1269260	Stress-activated protein kinase JNK	4.89	< 0.001
3	LOC1280522	Neuropeptide FF receptor 2	4.40	0.039
4	LOC4576208	Protein obstructor-E	4.15	< 0.001
5	LOC1271120	Protein regulator of cytokinesis 1	4.10	< 0.001
6	LOC1279262	CLIP domain-containing serine protease B15	4.10	< 0.001
7	LOC1269964	Chymotrypsin-2-like	3.99	0.007
8	LOC1270108	Uncharacterized	3.97	0.020
9	LOC1281383	Ninjurin-2	3.96	0.002
10	LOC1279267	CLIP domain-containing serine protease B15-like	3.89	0.002
11	LOC1277042	Uncharacterized	3.76	< 0.001
12	LOC133392142	Uncharacterized	3.62	0.030
13	LOC1271472	Uncharacterized	3.62	< 0.001
14	LOC4577422	Uncharacterized	3.43	< 0.001
15	LOC133393335	Uncharacterized	3.39	0.005
16	LOC133393411	Uncharacterized	3.33	0.001
17	LOC1280050	Annulin	3.27	< 0.001

18	LOC1269628	Monocarboxylate transporter 12	3.27	0.011
19	LOC1271676	Uncharacterized	3.18	< 0.001
20	LOC1277959	UDP-glucosyltransferase 2	3.12	< 0.001

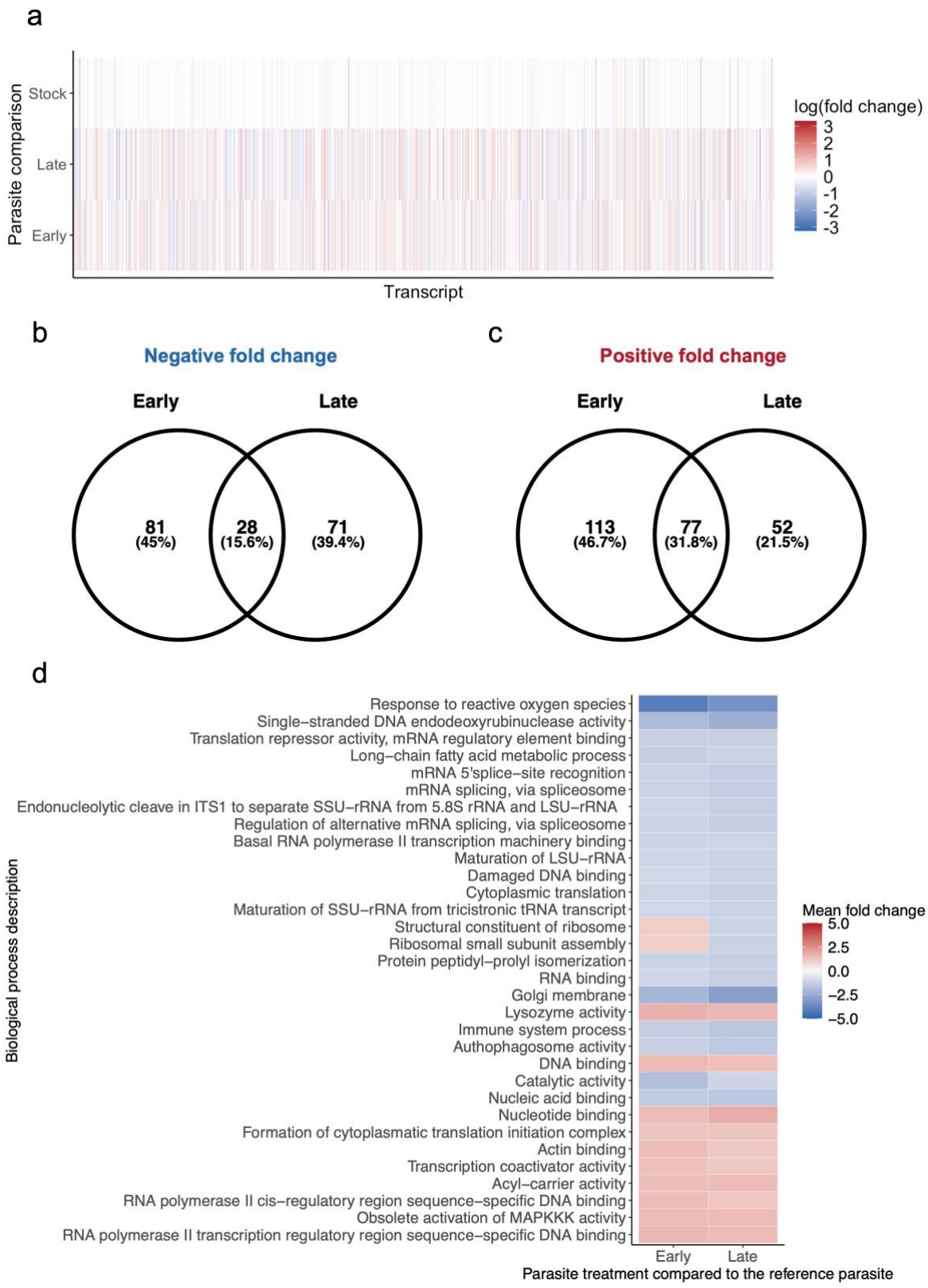

Figure 3. *Anopheles gambiae* transcriptional signatures of infection by *Vavraia culicis*. (a) Heatmap showing the log-transformed fold change in expression of all detected transcripts (i.e., 9920) by parasite (*Vavraia culicis*) treatment comparison. While the host *(Anopheles gambiae)* transcriptome in response to the *Stock* parasite was compared to the *Uninfected* host transcriptome, the response to *Early* and *Late* parasite treatments was compared to the response to the *Stock* parasite. A heatmap of all biological samples is presented in File S1, Figure S3. **(bc)** Venn diagrams showing the number of differentially expressed (DE) genes (adjusted p-value < 0.05) that are exclusively and commonly found between hosts infected with *Early* or *Late* parasites compared to the *Stock* parasite. Negative (b) and positive **(c)** differential expression are presented. **(d)** Heatmap illustrating mean fold change in expression per biological process families of significantly DE transcripts across all biological replicates of the same parasite treatment. Gene ontology annotation was performed using PANTHER 19.0 and VectorBase.

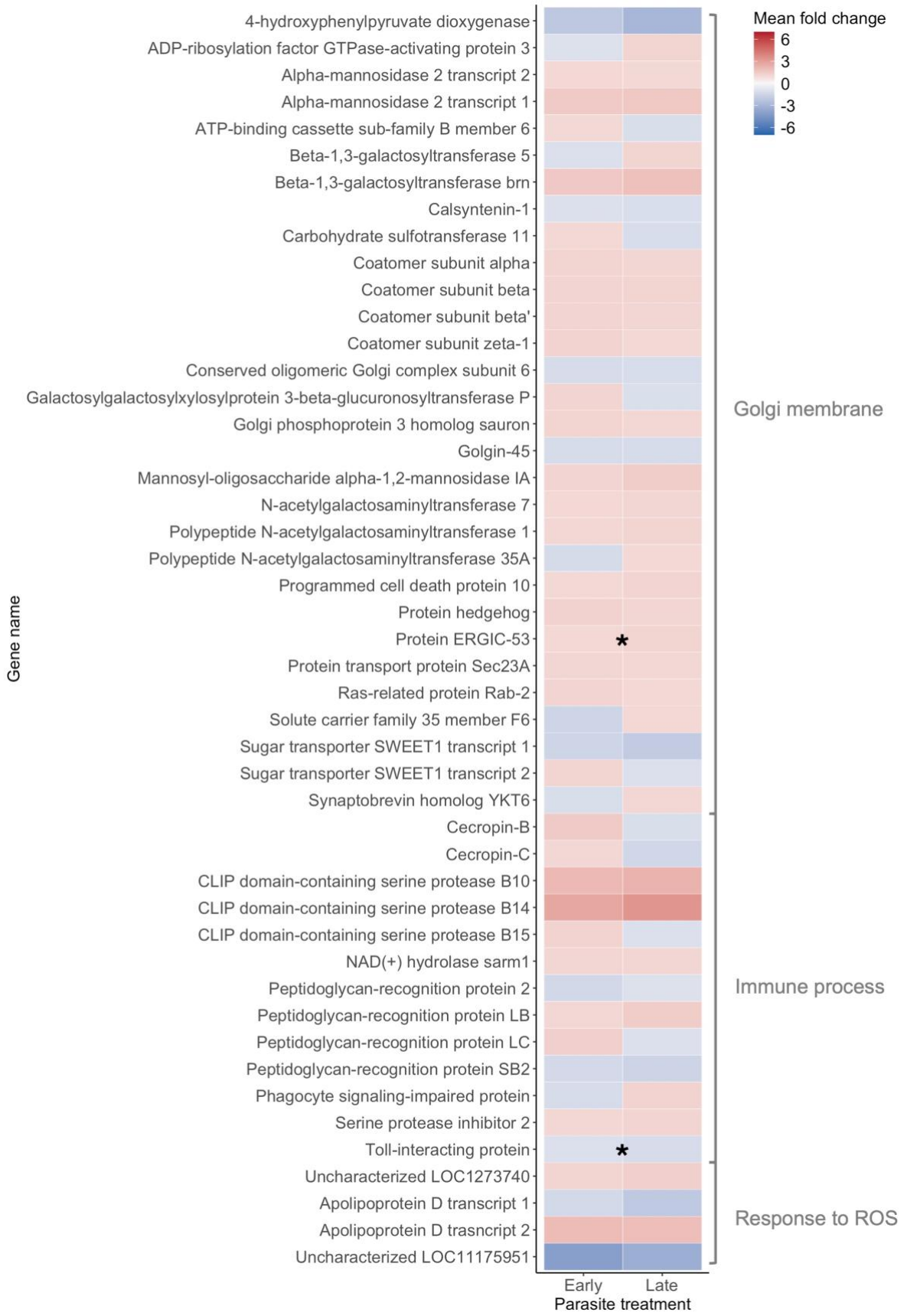
Mean fold change
6
3
0
-3
-6
4-hydroxyphenylpyruvate dioxygenase
ADP-ribosylation factor GTPase-activating protein 3
Alpha-mannosidase 2 transcript 2
Alpha-mannosidase 2 transcript 1
ATP-binding cassette sub-family B member 6
Beta-1,3-galactosyltransferase 5
Beta-1,3-galactosyltransferase brn
Calsyntenin-1
Carbohydrate sulfotransferase 11
Coatomer subunit alpha
Coatomer subunit beta
Coatomer subunit beta'
Coatomer subunit zeta-1
Conserved oligomeric Golgi complex subunit 6
Galactosylgalactosylxylosylprotein 3-beta-glucuronosyltransferase P
Golgi phosphoprotein 3 homolog sauron
Golgin-45
Mannosyl-oligosaccharide alpha-1,2-mannosidase IA
N-acetylgalactosaminyltransferase 7
Polypeptide N-acetylgalactosaminyltransferase 1
Polypeptide N-acetylgalactosaminyltransferase 35A
Programmed cell death protein 10
Protein hedgehog
Protein ERGIC-53
Protein transport protein Sec23A
Ras-related protein Rab-2
Solute carrier family 35 member F6
Sugar transporter SWEET1 transcript 1
Sugar transporter SWEET1 transcript 2
Synaptobrevin homolog YKT6
Cecropin-B
Cecropin-C
CLIP domain-containing serine protease B10
CLIP domain-containing serine protease B14
CLIP domain-containing serine protease B15
NAD(+) hydrolase sarm1
Peptidoglycan-recognition protein 2
Peptidoglycan-recognition protein LB
Peptidoglycan-recognition protein LC
Peptidoglycan-recognition protein SB2
Phagocyte signaling-impaired protein
Serine protease inhibitor 2
Toll-interacting protein
Uncharacterized LOC1273740
Apolipoprotein D transcript 1
Apolipoprotein D trasncript 2
Uncharacterized LOC11175951
Gene name
Golgi membrane
Immune process
Response to ROS
Early
Late
Parasite treatment

Figure 4. Differentially-expressed candidate genes during infection with selected parasites. Representation of the differentially-expressed candidate genes of the host *Anopheles gambiae* in response to infection by the microsporidian parasite *Vavraia culicis*. Fold difference in host expression of Golgi membrane (GO:0000139), response to reactive oxygen species (GO:0000302) and immune system process (GO:0002376) markers when compared to infection with the *Stock*. *Early* and *Late* selected fold change parasites were then compared to each other using a linear model (see Materials and Methods for details). Although the expression of all genes presented differed from the infection with *Stock* parasite, only the Toll-interacting and ERGIC-53 transcripts' fold change significantly differed between *Early* and *Late* parasites. *Late* had a lower expression of *Toll-interacting protein* ($df = 1$, $F = 9.70$, $p = 0.01$) and *protein ERGIC-53* ($df = 1$, $F = 7.69$, $p = 0.02$) than *Early* parasites, represented by an asterisk.

Results (909)

In this study, the *An. gambiae* transcriptome in response to unselected and selected lines of the microsporidian parasite *V. culicis* was characterized through RNA-seq. The findings suggest infection by each parasite treatment resulted in distinct transcriptomic profiles, which differed in their host immune response to each parasite. Moreover, the involvement of several biological processes, namely Golgi apparatus-associated signalling and response to reactive oxygen species (ROS), was also observed. The following sections describe and discuss these and other findings in detail.

Transcriptional profiles were measured on day 10 of mosquito adulthood, as a previous study has identified this as the time when all *V. culicis* within infected mosquitoes reach 100% prevalence in spore production, regardless of the *V. culicis* line infecting them [25]. Hence, this time point was chosen because sporulation represents an increase in parasite numbers, and therefore, it should elicit a more evident host response to the parasite. Nevertheless, it is noteworthy that, on average, infection by different lines of the parasite reached 100% prevalence at slightly different days of adulthood - i.e., *Stock* at day 10, *Early* at day 8 and *Late* at day 4.

Across the twelve samples (i.e., one *Uninfected*, one *Stock,* infected with unselected *V. culicis*, five *Early*, infected by five biological replicates for early transmission, and five *Late*, infected by five biological replicates for late transmission), 20 to 38 million reads were obtained, covering over 9,900 genes. The reads were successfully aligned to the *An. gambiae* genome (File S1, Fig. S1), and quality control confirmed their validity (File S1, Fig. S2). The number of genes detected by treatment, biological, and technical replicates can be found in File S1, Table S1.

1. Mosquito response to infection with an unselected Stock of V. culicis

First, the host transcriptional profile of *An. gambiae* infected with the *Stock* parasite was compared to *Uninfected* controls (Fig. 2, Table 1). Out of the 9,900 annotated genes, 1,967 genes were differentially expressed between Stock-infected and uninfected mosquitoes, with 1,104 upregulated (11.1%), 863 downregulated (8.7%), and 8,032 (80.2%) showing no differential expression (DE).

Although a higher number of up-regulated genes was found, the down-regulated genes exhibited higher fold changes (Table 1). For instance, the most down-regulated gene was the *Putative uncharacterized protein DDB_G0271606*, with a negative fold change of 1680.95. In contrast, the most up-regulated gene was an uncharacterized gene with a positive fold change of 13.30. Notably, upregulated genes included known immune effectors such as cecropin-B and ninjurin-2, while downregulated genes included CIMAP1D and arginine kinase 1, involved in sensory function and energy metabolism, respectively. Enriched GO categories included immune response, metabolic processes, and oxidative stress signalling, indicating a broad physiological shift in response to microsporidian infection (Fig. 2; Table 1). A complete list of the transcripts for this comparison is available in File S2. Next, the focus turned to comparing to *Uninfected* controls. The 20 most up- and down-regulated transcripts are listed in Table 1.

2. Mosquito response to infection by selected lines of V. culicis

Next, the DE profiles of *An. gambiae* infected by *Early* and *Late* parasite lines were also analyzed and compared to mosquitoes infected with *Stock V. culicis* (Fig. 3). A heatmap showing the expression of all transcripts across the different parasite lines shows a high fold-change in response to infection by selected parasites (i.e., *Early* and *Late*) compared to a standard infection by the *Stock* (even when this is compared to the *Uninfected* treatment) (Fig. 3a). Overall, Figure 3a demonstrates distinct expression profiles across the different parasite treatments. After comparing transcript expression to the reference *Stock*, transcripts that were uniquely DE in each selected treatment and those shared between treatments were identified (Fig. 3bc).

For down-regulated genes, 109 genes were poorly expressed by *Early* parasites. In comparison, 99 genes were down-regulated by *Late* parasites, with 28 genes commonly down-regulated in both treatments (Fig. 3b). For up-regulated genes, 190 genes were up-regulated in *Early* parasites, compared to 129 in *Late* parasites, with 77 genes commonly up-regulated in both groups (Fig. 3c). These findings suggest that a higher number of DE genes are found in response to infection by *Early* parasites compared to late-selected ones, at least during the 10th day of host adulthood. However, a notable overlap exists between both treatments (Fig. 3bc).

After categorizing the DE genes into their respective biological processes using Gene Ontology (GO) categories, a heatmap was plotted to display the mean fold change for each GO category across parasite treatments (Fig. 3d). Most categories exhibited similar fold changes between *Early* and *Late* parasites. However, three categories stood out as potential candidates for explaining differences between the two selected treatments due to their distinct expression patterns and biological relevance: response to reactive oxygen species (ROS), Golgi membrane, and immune system processes.

Genes with DE and their respective fold-change relative to the *Stock* were plotted for each candidate GO category (Fig. 4). The Golgi membrane category had the highest number of DE genes, and it showed the greatest variation between *Early* and *Late* parasites, followed by the immune process and response to ROS categories. Fold-change differences between the selected treatments were also compared. Only two genes showed significant differences: *Protein ERGIC-53* (df = 1, F = 7.69, p = 0.02; Golgi membrane) and *Toll-interacting protein* (df = 1, F = 9.70, p = 0.01; Immune process). Both genes had a higher fold change in *Late* parasites than in *Early* ones. However, while *Protein ERGIC-53* was up-regulated, *Toll-interacting protein* was down-regulated (Fig. 4).

Discussion (2112)

This study aims to provide a brief foundational description of the *An. gambiae* response to the microsporidian parasite *V. culicis*. To accomplish this, the host response was described and discuss in respect to infection by: i) an unselected microsporidian *V. culicis* (*Stock*), as well as ii) differently selected lines of the same microsporidian species, five selected for early transmission (*Early*) and five for late transmission (*Late*) within the same mosquito host (Fig. 1). The findings discussed below provide key insights into this host-parasite interaction and might have consequences for this vector's competence upon co-infection with *Plasmodium spp*.

1. Mosquito response to infection with an unselected Stock of V. culicis

When the *An. gambiae* transcriptomic response to infection by *Stock* was compared (Fig. 2, Table 1) to uninfected mosquitoes, a large number of differentially expressed (DE) genes were identified (see File S2 for the complete list of transcripts and their respective expression levels and file S3 for a list of the genes for this specific comparison). A broad response to infection by *V. culicis* has been previously reported in another mosquito species, the yellow-fever mosquito, *Ae. aegypti* [33]. Desjardins and colleagues conducted RNA-sequencing of two microsporidian parasites—*Vavraia culicis* (a generalist) and *Edhazardia aedis* (a specialist)—across two mosquito hosts (*Anopheles quadrimaculatus* and *Ae. aegypti*). They reported diverging host immune investment and pathogen transcriptional strategies. Similar to our results in *An. gambiae*, the authors found that *V. culicis* induces an upregulation of the

mosquito immune effectors, such as antimicrobial defensins. However, our study further reveals a broader transcriptional footprint, including Golgi apparatus activity, oxidative stress response, and metabolic processes—pathways not emphasized in Desjardins et al. (2015). These findings may contrast and stem from differences in sampling time points or infection stages. While Desjardins et al. (2015) primarily focus on intracellular pathogen dynamics across larval and adult transitions, our study captures sporulation at day 10 of adulthood. Together, these findings suggest that while certain immune elements, such as defensins and serine proteases, represent conserved responses to *V. culicis*, the overall magnitude and breadth of the host response are contingent upon host species, infection stage, and sampling design. This differential immunity phenotype between *Anopheles* and *Aedes* species has been demonstrated by Zeferino and Koella (2024), who observed that, *Ae. aegypti* mosquitoes clear the infection, whereas *An. gambiae* mosquitoes do not [24]. These host-parasite genotype-to-genotype associations are commonly found in nature, resulting from the evolutionary and ecological overlap between host and parasite, and are a key property of infection [36, 37].

Nevertheless, only a small fraction of the host genome was DE, with unclassified genes leading the numbers, followed by genes associated with biological and cellular processes and several other metabolic gene ontology categories (Fig. 2). Overall, metabolic and biosynthetic processes were some of the most well-represented, which likely suggests changes in the transcriptional response linked to the energy processing and translation of immune- and non-immune elements. From the immunity-related elements, only a few DE markers were identified, with two being notably overexpressed: *Cecropin-B*, an antimicrobial peptide known for its fungicidal properties *in vitro* [38, 39], and *Ninjurin-2*, a non-apoptotic cell death protein induced by the Toll pathway that plays a key role in the dipteran response to microbial infections [40, 41].

Significant over-expression of regeneration markers was also detected. For instance, *Annulin* was found to be responsible for peritrophic matrix formation in the gut and early resilience to infection [42], and *Obstructor-E*, a member of a multigene family, was shown to regulate insect cuticle development [43]. Additionally, *Rab11*, essential for the internalization of circulatory iron, was overexpressed [44], further validating previous findings on the role of iron during infection with *V. culicis*, where iron sequestration by the parasite has been hypothesized [45].

An overall downregulation of sensory genes was observed, including *Prestin*, which increases gut pH [46], and *CIMAP1D*, involved in sound-sensory function [47]. *Arginine kinase 1*, known to participate in ATP-to-ADP conversion and consequent energy release in certain bacteria [48], was found to be severely down-regulated in infected mosquitoes (Table 1). Interestingly, most Mucin proteins were up-regulated, except for *Mucin-6*, which was down-regulated. Mucin proteins are recognized for their role in epithelial lubrication, immune modulation and inflammation [49, 50]. Notably, *Mucin-6* is exclusive to the *An. gambiae* gut, which protects against parasites such as *Plasmodium spp* [51].

2. Mosquito response to infection by selected lines of V. culicis

Next, the focus is turned to how the host *An. gambiae* responds to parasite lines that were previously selected for early or late transmission within this mosquito species[25] (Fig. 3 and 4, File S2 and S4-13 for the gene comparisons between selected and unselected parasites). As expected, the number of differentially expressed (DE) genes was lower when comparing *Early* or *Late* parasites to *Stock*, relative to the broader contrast between *Stock* and *Uninfected* mosquitoes (299 and 228 *vs*. 1967 genes, respectively). As shown in the heatmap (Fig. 3a), both Early and Late parasite infections exhibit distinct expression profiles compared to the Stock, despite sharing a common host background. A higher number of DE genes was observed in response to *Early* parasites than *Late* ones, when compared to the *Stock*. However, there was a substantial overlap in expression patterns across the two parasite treatments (Fig. 3bc). To better understand the differences in transcriptomic profiles from infections with selected parasites, DE genes were categorized into biological processes using GO analysis (Fig. 3d). Most of the differences between *Early* and *Late* parasites were grouped into three GO biological processes: Golgi membrane, immune processes, and response to reactive oxygen species (ROS). These findings are unsurprising, given the biological relevance of these categories for infection [52–54], particularly from the host's perspective. Equally interestingly, the distinct host transcriptomic profile observed in response to infection between the *Early* and *Late* parasites indicates that selection did affect not only phenotypic traits, as shown in previous studies [25, 29, 45], but also drove significant parasite evolution, causing a substantial shift in the host's response to the selected parasites (Fig. 3 and 4).

The three GO categories mentioned above (i.e., Golgi membrane, immune processes, and response to ROS) were treated as candidate categories, along with their associated genes, which are believed to play crucial roles in modulating host-parasite dynamics and therefore warrant further study (Fig. 4). First, the Golgi membrane was considered, as it has recently gained attention for its critical role in innate immune signalling, preceding other organelles such as mitochondria and the endoplasmic reticulum (ER) during infection [52]. As a result, the apparent difference observed in the host response to *Early* or *Late* parasite treatments was unsurprising (Fig. 3). The genes associated with the Golgi membrane include coatomers, galactosyltransferases, and mannosidases, which are involved in vesicle transport and carbohydrate metabolism with the ER. The richness and differential expression of Golgi membrane-associated genes suggest that some upregulation of effectors involved in glycosylation and trafficking processes in the Golgi apparatus occurs across both parasite treatments (Fig. 4).

One gene, *ERGIC-53*, stood out due to its significantly different fold-change between host responses to infections by *Early* and *Late* parasites. The protein encoded by *ERGIC-53* is involved in the trafficking of glycoproteins. The *Early* parasites seem to induce higher production of ERGIC-53 and, consequently, this suggests an increased investment in glycoprotein trafficking compared to *Late* (Fig. 4). Although

the precise role of ERGIC-53 in the immune response of *An. gambiae* remains unclear, it can be hypothesized, based on existing literature, that glycoproteins (e.g., peptidoglycan recognition proteins or PGRPs) serve as essential information markers for the host, vital for accurate recognition and elimination of parasites [55, 56]. Nevertheless, it is essential to note that further studies are needed to validate such claims. Statistical changes in these effectors do not mean they are themselves involved in the process/changes, but instead might be the pathway they are in.

Second, variation in the expression of immune-related genes was analyzed, including *peptidoglycan-recognition proteins* (PGRPs), *CLIP domain serine proteases* and *cecropins*, among others (Fig. 3). A notable difference was observed between the host response to *Early* and *Late* parasite treatments, with many of the DE immune-related genes being downregulated upon infection with *Late* parasites (Fig. 3). Interestingly, both *cecropin-B* and *cecropin-C* were overexpressed in response to early-selected parasites compared to *Stock*, suggesting a more robust antimicrobial response. However, this pattern was not observed in response to *Late* parasites, but rather the opposite. In particular, *CLIP domain serine proteases* have been associated with mosquito late resistance to *Plasmodium* via melanisation [57, 58] (Table 1, Fig. 4). In this study, I noticed all lines of *V. culicis* induced an up-regulation of these immune effectors, suggesting that infection by this microsporidian might elicit an immune response that has collateral damage to *Plasmodium* development.

Although it was hypothesized that the immune response to *Late* parasites would be stronger due to their higher virulence, time, and replication within the host, the data might suggest otherwise. Two hypotheses are proposed to explain this finding, although they are merely speculative at this stage.

The first hypothesis involves recognizing *V. culicis* as a virulent parasite. As discussed in the manuscript, *Early* parasites induce a larger Golgi membrane response, potentially leading to better recognition of PGRPs than infection by Late parasites. This could explain the rapid up-regulation of immune markers in response to *Early* parasites. The second hypothesis concerns the balance between the costs and benefits of the immune response and its association with the presence/absence of damage-associated molecular patterns (DAMPs) [59]. As with any other life history trait, investment in immunity is expected to trade off with other physiological traits [60]. As suggested by Rolff and Lazzaro (2012), the intensity and type of the immune response may result from the recognition of a combination of molecules, alerting the host to the parasite (PGRPs) and/or to the damage inflicted by the infection (DAMPs). If so, infection by the more virulent *Late* parasite could lead to a more costly and damaging infection, potentially overwhelming the host. In this scenario, the host may prioritize reproductive fitness over survival, which aligns with previous observations of increased reproductive investment during infection by *Late* parasites [25]. This phenomenon has been documented in various infections, as predicted by life history theory [60]. In extreme cases, the investment shift to fecundity can be lifelong due to the host's shortened lifespan. In this specific case, we refer to this phenomenon as

terminal investment, which may occur when a host invests its resources into fecundity due to an inability to survive the infection [61–63]. It is unclear whether this shift in fecundity and immunity is temporary or observed throughout the host's life, given that both fecundity and RNA-seq were performed at the same infection time point and did not represent the entire infection process. It is noteworthy to say that the individuals in this study were not blood-fed, which is necessary for their reproduction. Although we cannot confirm there is a trade-off with fecundity or other life history traits, we are aware *An. gambiae* invests in its first clutch of eggs before having a blood meal, which would represent at least a partial investment in fecundity. Moreover, from this category, the *Toll-interacting protein* was found to have significantly different fold changes between the infection by each of the two selection parasite treatments (Fig. 4). This gene, which produces a protein important for parasite recognition [64–67], was slightly more up-regulated in response to *Early* parasites than to *Late* ones (Fig. 4). This might support the idea that *Early* parasites may be more recognizable by the host's immune system. However, the extent to which parasite selection has affected the presence or absence of specific PGRPs that enable host recognition remains unclear.

It is essential to state the limitations of this study at this stage. Here, the aim is to provide the first description of the mosquito response to *V. culicis* and, potentially, other microsporidia by extension. However, the observations in this study are insufficient to fully understand parasite evolution, nor do they reflect in-depth mechanisms or how these mechanisms change with the progression of infection, which is particularly challenging in the presence of multiple lines of *V. culicis* with distinct growth cycles. Nevertheless, discussing potential scenarios is of interest and may pave the way for future research avenues.

Third, only a few genes were found to be DE in response to ROS, showing mixed expression patterns (Fig. 4). Overall, *Early* parasites elicited a stronger host response to ROS than *Late* ones, suggesting higher oxidative stress within the host. This is likely due to a heightened immune response to this infection. This ROS response emerges as a candidate axis of interaction that warrants further exploration in future time and tissue-specific studies.

Conclusions (447)

In conclusion, the transcriptional response of *An. gambiae* to infection by *V. culicis* has revealed curious and significant insights into this host-parasite interaction and its evolutionary history. Moreover, the findings in this study further explain many of the results measured in previous studies concerning the effects of selecting *V. culicis* for early and late transmission [25, 29, 45]. Differential expression of genes related to immune response, Golgi membrane function, and oxidative stress was observed, with distinct patterns emerging between infections with reference to *Stock*, *Early* and *Late* parasite lines.

Overall, *Early* parasites seemed to elicit a broader and more pronounced immune response, characterized by the upregulation of immune-related genes, such as cecropin and PGRPs, and enhanced glycoprotein trafficking through the Golgi apparatus. In contrast, *Late* parasites appeared to trigger a weaker immune response and, therefore, potentially evolved immune evasion mechanisms; however, such claims are still subject to testing.

Altogether, the results of this study demonstrate that selection pressures on *V. culicis* not only influence its phenotypic traits but also drive significant changes in the host gene expression, revealing complex host-parasite co-evolutionary dynamics. Further investigation is needed to elucidate and quantify the specific molecular mechanisms involved, particularly in relation to immune strategies and the balance between host survival and reproductive fitness. Additionally, it is essential to situate this study within the context of the microsporidian's capacity to interfere with *Plasmodium* development, as previously mentioned. Vector-borne parasites, such as *Plasmodium spp.*, transmitted by this host, have long transmission cycles within their vectors. It is reasonable to expect that co-infection of Plasmodium spp. and microsporidia may inadvertently select for late-transmitted microsporidian parasites, which could have significant consequences for the spread of both parasites within a population. Although the mechanism by which microsporidians suppress *Plasmodium* development remains unclear, our study demonstrated that melanization-based immunity is upregulated, which might facilitate late collateral melanization of *Plasmodium* oocysts. Nevertheless, this hypothesis remains to be tested, as, in addition to *CLIP proteases*, we observed a limited immune response that could impact *Plasmodium spp.* Consequently, resource competition between the parasites may be a primary source of this inhibitory relationship as well. Moreover, although conclusions must be taken with some consideration, the results suggest a lack of immunity towards late-transmitted *V. culicis, which* may highlight the potential of this parasite as a biological vector control, as it suggests that selection to reduce its prevalence in a population is low. Further research is needed to fully understand this interaction, but our study provides a foundation for it. These findings provide valuable insights that could inform future vector control strategies, particularly in the context of the evolutionary pressures exerted by parasites on mosquito populations and the diseases they vector.

Materials and Methods (1174)

1. Experimental model

The Kisumu strain of the mosquito host *Anopheles gambiae (s.s.)* and evolved lines of the microsporidian parasite *Vavraia culicis floridensis* were used for these experiments. These parasite lines had previously been selected for seven generations for: i) early transmission and shorter time within the host (i.e., *Early*); or for ii) late transmission and longer time within the host (i.e., *Late*); or iii) they come

from an unselected reference, our unselected laboratory stock (i.e., *Stock*) [25]. Further details on the selection experiment and its maintenance are described in Silva and Koella (2024). All experiments and rearing were conducted under standard laboratory conditions (26 ± 1º C, 70 ± 5% relative humidity, and 12 h light/dark cycle).

2. Experiment and samples collection

Freshly hatched *An. gambiae* larvae were reared in groups of 50 individuals per petri dish (120 mm diameter × 17 mm) containing 80 ml of distilled water. Larvae were fed daily with Tetramin Baby fish food according to their age: 0.04, 0.06, 0.08, 0.16, 0.32, and 0.6 mg/larva for 0, 1, 2, 3, 4, and 5 days or older, respectively. On the second day of larval development, individuals were exposed to 10,000 spores per larva of their respective *V. culicis* treatment, or not exposed in the case of the *Uninfected* treatment. At pupation, individuals were transferred into 50 ml falcon tubes with approximately 10 ml of distilled water and were allowed to emerge as adults. Female mosquitoes were transferred to individual cups containing humid filter paper and provided with a constant 6% sucrose solution until death. On day 10 of adulthood, all live female mosquitoes were collected, snap-frozen in liquid nitrogen, and stored at -80ºC until RNA extraction. Transcriptomic profiles were assessed at day 10 of adulthood, as previous studies on these lines have shown that this is when all hosts produce infective spores [25]. Thus, a stronger host response and more pronounced signatures of parasite selection were anticipated for this time point.

In total, 10 female mosquitoes were collected and processed per parasite treatment per line. The parasite line is then the biological replicate, where five independently selected lines are used for early or late transmission, or five biological replicates for the *Stock*. RNA was extracted from the pool of these 10 females for each treatment and line. After extraction, the same sample was measured four times, i.e., in four technical replicates. We then performed the statistical analyses described below at the biological replicate level.

3. RNA extractions

RNA extractions were performed using Qiagen's RNAeasy Universal Plus kit following the provided protocol. Before beginning the protocol, ten female mosquitoes per parasite treatment per line were pooled in a 1.5 mL microcentrifuge tube with 1000 µl of Qiazol reagent (from the RNAeasy Universal Plus kit by Qiagen), briefly mixed, and two stainless steel beads (Ø 2 mm) were added. Each tube was homogenized using a Qiagen TissueLyser LT at a frequency of 30 Hz for three minutes. The Qiagen kit protocol was then followed, resulting in a 50 µl eluted solution of RNA in nuclease-free water at a concentration of approximately 300 ng/µl for each treatment. RNA samples were standardized to 10

ng/µl and delivered on dry ice to the Genomic Technologies Facility (University of Lausanne, Switzerland) for further processing, as described below.

4. RNA sequencing

RNA quality was assessed using a Fragment analyzer (Agilent Technologies). The poly-A tails and adapters were removed from single-end reads, and quality was trimmed with Cutadapt version 4.8 [68]. Reads matching ribosomal RNA sequences were removed with fastq_screen version 0.11.1 [69]. Reads longer than 40nt were aligned against the concatenated genomes of *Anopheles gambiae* (NCBI: GCA_943734735.2) and *Vavraia culicis floridensis* (NCBI: GCA_000192795.1) using STAR version 2.7.10a [70]. The number of read counts per gene locus was summarized with htseq-count version 0.11.2 [71] using gene annotation. RNA-seq libraries were prepared from 250 ng of total RNA using the Illumina Stranded mRNA Prep reagents (Illumina) with a unique dual indexing strategy, following the official protocol, which was automated on a Sciclone liquid handling robot (PerkinElmer). Libraries were quantified by a fluorometric method (QubIT, Life Technologies), and their quality was assessed on a Fragment Analyzer (Agilent Technologies). Sequencing was performed on an Illumina NovaSeq 6000 for 150 cycles single read. Sequencing data were demultiplexed using the bcl2fastq2 Conversion Software (version 2.20, Illumina).

5. Statistical analysis

All the analyses were performed with R version 4.3.0. in RStudio version 3034.06.2+561. The following packages were used for the statistical analysis and diagnosis, and for visualising and plotting the data: "Glimma" [72], "cowplot" [73], "ggrepel" [74], "RColorBrewer" [75], "maptools" [76], "sp" [77], "edgeR" [78], "MASS" [79], "limma" [80], "knitr" [81], "ggplot2" [82] and "dplyr" [83]. Figure panels were created and edited with BioRender.com and Microsoft PowerPoint 16.16.27. The R Script for the statistical analyses and respective figures can be found in File S14. The respective data files are Files S15-20.

The high quality of the RNA-seq data alignment was verified using RSeQC version 5.0.1 [84]. Alignment rates to both genomes exceed 93.5% for all samples (File S1, Fig. S1a). A very small number of reads aligned to *V. culicis*, ranging from 127 to 5,393 (File S1, Fig. S1b). *An. gambiae* samples exhibit good sequencing depth (File S1, Fig. S1c) and diverse gene representation. The gene body coverage is biased towards the 3' end, suggesting partial RNA degradation, but this pattern is consistent across all samples.

Genes with low counts were filtered out according to the rule of 3 count(s) per million (cpm) in at least 4 sample(s). Library sizes were scaled using TMM normalization and log-transformed into counts per million or CPM (EdgeR package version 3.42.4) [78]. Statistical quality controls were performed through density gene expression distribution, clustering, and sample PCA (File S1, Fig. S2). Differential expression was computed with limma-trend approach [80] by fitting all samples into one linear model. Next, the following group of comparisons were performed:

- Infected with *Stock vs. Uninfected* (1 comparison).
- Infected with selected parasite *vs.* infected with *Stock* (10 comparisons, one for each parasite line).

A moderated t-test was used for each contrast. The Benjamini-Hochberg method computed an adjusted p-value for each comparison, controlling for false discovery rate (FDR, Adj. p). Then, a host gene ontology (GO) enrichment analysis was carried out on differentially expressed (DE) genes through Panther 19.0 and "vectorbase.org" using the *An. gambiae* genome as a reference (Fig. 2-4). The host response to different biological replicate lines of *Early* and *Late* were then pooled together per selection treatment, and their average expression, compared to *Stock*, was calculated and plotted.

Afterwards, a candidate gene analysis was performed (Fig. 4) considering the differently expressed biological processes in selected parasites, comparatively to *Stock* (Fig. 3). For each DE transcript of the GO:0000139 (Golgi membrane), GO:0000302 (Response to reactive oxygen species) and GO:0002376 (Immune system process) classes, a linear model was run with fold-change as a dependent variable and parasite treatment as an explanatory variable. These comparisons enable us to test for differential fold changes (compared to the *Stock*) for *Early* and *Late* parasites.

Author contributions

LMS designed and conducted the experiments, analyzed the data and wrote the manuscript.

Acknowledgements

I thank Tiago G. Zeferino, Paula Escuer Pifarré, and Amjad Khalaf for their advice and experimental support. I also thank the Lausanne Genomic Technologies Facility (University of Lausanne, Switzerland) team, including Johann Weber, Julien Marquis, Sandra Calderon Copete, and Viviane Praz, for their assistance with library preparation, sequencing, and data analysis. I especially thank Jacob C. Koella for constant feedback, support, and critical comments on the first draft of the

manuscript. The project was supported by the Basler Stiftung für biologische Forschung and LMS by SNF grant 310030_192786.

Competing interests

The author declares that they have no competing interests.

References

1. Silva LM, Acerbi G, Amann M, Koella JC. Exposure to Pseudomonas spp. increases Anopheles gambiae insecticide resistance in a host-dependent manner. Sci Rep. 2024;14:29789.
2. Ranasinghe HAK, Amarasinghe LD. Naturally occurring microbiota associated with mosquito breeding habitats and their effects on mosquito larvae. Biomed Res Int. 2020;2020.
3. Dong Y, Manfredini F, Dimopoulos G. Implication of the mosquito midgut microbiota in the defense against malaria parasites. PLoS Pathog. 2009;5:e1000423.
4. Caragata EP, Tikhe C V, Dimopoulos G. Curious entanglements: interactions between mosquitoes, their microbiota, and arboviruses. Curr Opin Virol. 2019;37:26–36.
5. Duncan AB, Agnew P, Noel V, Michalakis Y. The consequences of co-infections for parasite transmission in the mosquito A edes aegypti. J Anim Ecol. 2015;84:498–508.
6. Bozic J, Capone A, Pediconi D, Mensah P, Cappelli A, Valzano M, et al. Mosquitoes can harbour yeasts of clinical significance and contribute to their environmental dissemination. Environ Microbiol Rep. 2017;9:642–8.
7. Becnel JJ, Weiss LM. Microsporidia: pathogens of opportunity. John Wiley & Sons Incorporated; 2014.
8. Herren JK, Mbaisi L, Mararo E, Makhulu EE, Mobegi VA, Butungi H, et al. A microsporidian impairs Plasmodium falciparum transmission in Anopheles arabiensis mosquitoes. Nat Commun. 2020;11:1–10.
9. Bjørnson S, Oi D. Microsporidia biological control agents and pathogens of beneficial insects. Microsporidia Pathog Oppor. 2014;:635–70.
10. Franzen C. Microsporidia: a review of 150 years of research. Open Parasitol J. 2008;2.
11. Seatamanoch N, Kongdachalert S, Sunantaraporn S, Siriyasatien P, Brownell N. Microsporidia, a highly adaptive organism and its host expansion to humans. Front Cell Infect Microbiol. 2022;12:924007.
12. Keeling PJ, Fast NM, Law JS, Williams BAP, Slamovits CH. Comparative genomics of microsporidia. Folia Parasitol (Praha). 2013;52:8–14.
13. Keesey IW, Koerte S, Khallaf MA, Retzke T, Guillou A, Grosse-Wilde E, et al. Pathogenic

bacteria enhance dispersal through alteration of Drosophila social communication. Nat Commun. 2017;8:265.
14. Keeling PJ, Fast NM. Microsporidia: biology and evolution of highly reduced intracellular parasites. Annu Rev Microbiol. 2002;56:93–116.
15. Silva LM, Zeferino TG, Koella JC. Vavraia culicis. Trends Parasitol. 2025. https://doi.org/https://doi.org/10.1016/j.pt.2025.02.011.
16. Koella JC, Saddler A, Karacs TPS. Blocking the evolution of insecticide-resistant malaria vectors with a microsporidian. Evol Appl. 2012;5:283–92.
17. Koella JC, Lorenz L, Bargielowski I. Microsporidians as evolution-proof agents of malaria control? Adv Parasitol. 2009;68:315–27.
18. Bargielowski I, Koella JC. A possible mechanism for the suppression of Plasmodium berghei development in the mosquito Anopheles gambiae by the microsporidian Vavraia culicis. PLoS One. 2009;4:e4676.
19. Kelly JF, Anthony DW, Dillard CR. A laboratory evaluation of the microsporidian Vavraia culicis as an agent for mosquito control. J Invertebr Pathol. 1981;37:117–22.
20. Lorenz LM, Koella JC. The microsporidian parasite Vavraia culicis as a potential late life–acting control agent of malaria. Evol Appl. 2011;4:783–90.
21. Vyas-Patel N. The Suppression of Plasmodium berghei in Anopheles coluzzii infected later with Vavraia culicis. bioRxiv. 2023;:2002–23.
22. Makhulu EE, Onchuru TO, Gichuhi J, Otieno FG, Wairimu AW, Muthoni JN, et al. Localization and tissue tropism of the symbiont Microsporidia MB in the germ line and somatic tissues of Anopheles arabiensis. MBio. 2024;15:e02192-23.
23. Bukhari T, Pevsner R, Herren JK. Microsporidia: a promising vector control tool for residual malaria transmission. Front Trop Dis. 2022;3:957109.
24. Zeferino TG, Koella JC. Host-specific effects of a generalist parasite of mosquitoes. Sci Rep. 2024;14:18365.
25. Silva LM, Koella JC. Complex interactions in the life cycle of a simple parasite shape the evolution of virulence. PLoS Pathog. 2025. https://doi.org/https://doi.org/10.1371/journal.ppat.1013294.
26. Sy VE, Agnew P, Sidobre C, Michalakis Y. Reduced survival and reproductive success generates selection pressure for the dengue mosquito Aedes aegypti to evolve resistance against infection by the microsporidian parasite Vavraia culicis. Evol Appl. 2014;7:468–79.
27. Vyas-Patel N. Anopheles coluzzii infection by the microsporidian, Vavraia culicis: the effect of host age. bioRxiv. 2020;:2010–20.
28. Khalaf A, Francis O, Blaxter ML. Genome evolution in intracellular parasites: Microsporidia and Apicomplexa. J Eukaryot Microbiol. 2024;:e13033.
29. Silva LM, Koella JC. Virulence evolution: thinking outside of the host. bioRxiv. 2024;:2005–24.

30. Nakjang S, Williams TA, Heinz E, Watson AK, Foster PG, Sendra KM, et al. Reduction and expansion in microsporidian genome evolution: new insights from comparative genomics. Genome Biol Evol. 2013;5:2285–303.
31. Yassine H, Osta MA. Anopheles gambiae innate immunity. Cell Microbiol. 2010;12:1–9.
32. Osta MA, Christophides GK, Vlachou D, Kafatos FC. Innate immunity in the malaria vector Anopheles gambiae: comparative and functional genomics. J Exp Biol. 2004;207:2551–63.
33. Desjardins CA, Sanscrainte ND, Goldberg JM, Heiman D, Young S, Zeng Q, et al. Contrasting host–pathogen interactions and genome evolution in two generalist and specialist microsporidian pathogens of mosquitoes. Nat Commun. 2015;6:7121.
34. Kanost MR, Jiang H. Clip-domain serine proteases as immune factors in insect hemolymph. Curr Opin insect Sci. 2015;11:47–55.
35. Waterhouse RM, Kriventseva E V, Meister S, Xi Z, Alvarez KS, Bartholomay LC, et al. Evolutionary dynamics of immune-related genes and pathways in disease-vector mosquitoes. Science (80-). 2007;316:1738–43.
36. Duneau D, Ferdy J-B, Revah J, Kondolf H, Ortiz GA, Lazzaro BP, et al. Stochastic variation in the initial phase of bacterial infection predicts the probability of survival in D. melanogaster. Elife. 2017;6.
37. Acuña-Hidalgo B, Silva LM, Franz M, Regoes RR, Armitage SAO. Decomposing virulence to understand bacterial clearance in persistent infections. Nat Commun. 2022;13:1–14.
38. De Lucca AJ, Bland JM, Jacks TJ, Grimm C, Walsh TJ. Fungicidal and binding properties of the natural peptides cecropin B and dermaseptin. Med Mycol. 1998;36:291–8.
39. De Lucca AJ, Bland JM, Vigo CB, Jacks TJ, Peter J, Walsh TJ. D-cecropin B: proteolytic resistance, lethality for pathogenic fungi and binding properties. Med Mycol. 2000;38:301–8.
40. Broderick S, Wang X, Simms N, Page-McCaw A. Drosophila Ninjurin A induces nonapoptotic cell death. 2012.
41. Thomas T, De T Das, Sharma P, Verma S, Rohilla S, Pandey KC, et al. Structural and functional prediction analysis of mosquito Ninjurin protein: Implication in the innate immune responses in Anopheles stephensi. Int J Mosq Res. 2014;1:60–5.
42. Wang Z, Wilhelmsson C, Hyrsl P, Loof TG, Dobes P, Klupp M, et al. Pathogen entrapment by transglutaminase—a conserved early innate immune mechanism. PLoS Pathog. 2010;6:e1000763.
43. Behr M, Hoch M. Identification of the novel evolutionary conserved obstructor multigene family in invertebrates. FEBS Lett. 2005;579:6827–33.
44. Wilcke M, Johannes L, Galli T, Mayau V, Goud B, Salamero J. Rab11 regulates the compartmentalization of early endosomes required for efficient transport from early endosomes to the trans-golgi network. J Cell Biol. 2000;151:1207–20.
45. Silva LM, Vallat A, Koella JC. Mechanisms of host exploitation by a microsporidian parasite. Proc R Soc B. 2025. https://doi.org/https://doi.org/10.1098/rspb.2025.1123.

46. Hirata T, Czapar A, Brin L, Haritonova A, Bondeson DP, Linser P, et al. Ion and solute transport by Prestin in Drosophila and Anopheles. J Insect Physiol. 2012;58:563–9.
47. Senthilan PR, Piepenbrock D, Ovezmyradov G, Nadrowski B, Bechstedt S, Pauls S, et al. Drosophila auditory organ genes and genetic hearing defects. Cell. 2012;150:1042–54.
48. Cozzone AJ. ATP-dependent protein kinases in bacteria. J Cell Biochem. 1993;51:7–13.
49. Dam TK, Brewer CF. Multivalent lectin—carbohydrate interactions: energetics and mechanisms of binding. Adv Carbohydr Chem Biochem. 2010;63:139–64.
50. Kufe DW. Mucins in cancer: function, prognosis and therapy. Nat Rev Cancer. 2009;9:874–85.
51. Shen Z, Dimopoulos G, Kafatos FC, Jacobs-Lorena M. A cell surface mucin specifically expressed in the midgut of the malaria mosquito Anopheles gambiae. Proc Natl Acad Sci. 1999;96:5610–5.
52. Tao Y, Yang Y, Zhou R, Gong T. Golgi apparatus: an emerging platform for innate immunity. Trends Cell Biol. 2020;30:467–77.
53. Bahia AC, Oliveira JHM, Kubota MS, Araújo HRC, Lima JBP, Rios-Velasquez CM, et al. The role of reactive oxygen species in Anopheles aquasalis response to Plasmodium vivax infection. PLoS One. 2013;8:e57014.
54. Andreyev AY, Kushnareva YE, Starkova NN, Starkov AA. Metabolic ROS signaling: to immunity and beyond. Biochem. 2020;85:1650–67.
55. Davicino RC, Eliçabe RJ, Di Genaro MS, Rabinovich GA. Coupling pathogen recognition to innate immunity through glycan-dependent mechanisms. Int Immunopharmacol. 2011;11:1457–63.
56. Sperandio M, Gleissner CA, Ley K. Glycosylation in immune cell trafficking. Immunol Rev. 2009;230:97–113.
57. Zhang X, Li M, El Moussawi L, Saab S, Zhang S, Osta MA, et al. CLIPB10 is a terminal protease in the regulatory network that controls melanization in the African malaria mosquito Anopheles gambiae. Front Cell Infect Microbiol. 2021;10:585986.
58. Zeineddine S, Jaber S, Saab SA, Nakhleh J, Dimopoulos G, Osta MA. Late sporogonic stages of Plasmodium parasites are susceptible to the melanization response in Anopheles gambiae mosquitoes. Front Cell Infect Microbiol. 2024;14.
59. Lazzaro BP, Rolff J. Danger, microbes, and homeostasis. Science (80-). 2011;332:43–4.
60. Stearns SC. Trade-offs in life-history evolution. Funct Ecol. 1989;3:259–68.
61. Hudson AL, Moatt JP, Vale PF. Terminal investment strategies following infection are dependent on diet. J Evol Biol. 2020;33:309–17.
62. Clutton-Brock TH. Reproductive effort and terminal investment in iteroparous animals. Am Nat. 1984;123:212–29.
63. Duffield KR, Bowers EK, Sakaluk SK, Sadd BM. A dynamic threshold model for terminal investment. Behav Ecol Sociobiol. 2017;71:1–17.
64. Burns K, Clatworthy J, Martin L, Martinon F, Plumpton C, Maschera B, et al. Tollip, a new

component of the IL-1RI pathway, links IRAK to the IL-1 receptor. Nat Cell Biol. 2000;2:346–51.
65. Zhang G, Ghosh S. Negative regulation of toll-like receptor-mediated signaling by Tollip. J Biol Chem. 2002;277:7059–65.
66. Didierlaurent A, Brissoni B, Velin D, Aebi N, Tardivel A, Käslin E, et al. Tollip regulates proinflammatory responses to interleukin-1 and lipopolysaccharide. Mol Cell Biol. 2006.
67. Valanne S, Wang J-H, Rämet M. The Drosophila toll signaling pathway. J Immunol. 2011;186:649–56.
68. Martin M. Cutadapt removes adapter sequences from high-throughput sequencing reads. EMBnet J. 2011;17:10–2.
69. Wingett SW, Andrews S. FastQ Screen: A tool for multi-genome mapping and quality control. F1000Research. 2018;7.
70. Dobin A, Davis CA, Schlesinger F, Drenkow J, Zaleski C, Jha S, et al. STAR: ultrafast universal RNA-seq aligner. Bioinformatics. 2013;29:15–21.
71. Anders S, Pyl PT, Huber W. HTSeq—a Python framework to work with high-throughput sequencing data. bioinformatics. 2015;31:166–9.
72. Su S, Law CW, Ah-Cann C, Asselin-Labat M-L, Blewitt ME, Ritchie ME. Glimma: interactive graphics for gene expression analysis. Bioinformatics. 2017;33:2050–2.
73. Wilke CO, Wickham H, Wilke MCO. Package 'cowplot.' Streamlined plot theme plot Annot 'ggplot2. 2019;1.
74. Slowikowski K, Schep A, Hughes S, Lukauskas S, Irisson J-O, Kamvar ZN, et al. Package ggrepel. Autom position non-overlapping text labels with 'ggplot2. 2018.
75. Neuwirth E, Neuwirth ME. Package 'RColorBrewer.' CRAN 2011-06-17 08: 34: 00. Apache License 2.0; 2011.
76. Bivand R, Lewin-Koh N, Pebesma E, Archer E, Baddeley A, Bearman N, et al. Package 'maptools.' Packag 'maptools.' 2023.
77. Pebesma E, Bivand R, Pebesma ME, RColorBrewer S, Collate AAA. Package 'sp.' Compr R Arch Netw. 2012;9.
78. Robinson MD, McCarthy DJ, Smyth GK. edgeR: a Bioconductor package for differential expression analysis of digital gene expression data. bioinformatics. 2010;26:139–40.
79. Ripley B, Venables B, Bates DM, Hornik K, Gebhardt A, Firth D, et al. Package 'mass.' Cran r. 2013;538:113–20.
80. Ritchie ME, Phipson B, Wu DI, Hu Y, Law CW, Shi W, et al. limma powers differential expression analyses for RNA-sequencing and microarray studies. Nucleic Acids Res. 2015;43:e47–e47.
81. Xie Y. knitr: a comprehensive tool for reproducible research in R. In: Implementing reproducible research. Chapman and Hall/CRC; 2018. p. 3–31.
82. Wickham H. ggplot2: elegant graphics for data analysis. springer; 2016.

83. Wickham H, François R, Henry L, Müller K, Wickham MH. Package 'dplyr.' A Gramm Data Manip R Packag version. 2019;8.
84. Wang L, Wang S, Li W. RSeQC: quality control of RNA-seq experiments. Bioinformatics. 2012;28:2184–5.

Supplementary information

File S1. Supplementary information document. This document includes the following tables/figures:

Table S1. Number of genes annotated per sample.

Figure S1. Host RNA-sequencing and parasite gene counts.

Figure S2. Quality control clustering and PCAs.

Figure S3. Heatmap of the complete host transcriptome in response to each parasite treatment and biological replicate.

File S2. Expression of all detected transcripts by parasite treatment, biological replicate and technical replicate.

File S3. Transcript expression and statistical contrasts for *Stock* infection *vs. Uninfected*.

File S4. Transcript expression and statistical contrasts for *Early* (biological replicate 1) infection *vs. Stock* infection.

File S5. Transcript expression and statistical contrasts *Early* (biological replicate 2) infection *vs. Stock* infection.

File S6. Transcript expression and statistical contrasts for *Early* (biological replicate 3) infection *vs. Stock* infection.

File S7. Transcript expression and statistical contrasts for *Early* (biological replicate 4) infection *vs. Stock* infection.

File S8. Transcript expression and statistical contrasts for *Early* (biological replicate 5) infection *vs. Stock* infection.

File S9. Transcript expression and statistical contrasts for *Late* (biological replicate 1) infection *vs. Stock* infection.

File S10. Transcript expression and statistical contrasts for *Late* (biological replicate 2) infection *vs. Stock* infection.

File S11. Transcript expression and statistical contrasts for *Late* (biological replicate 3) infection *vs. Stock* infection.

File S12. Transcript expression and statistical contrasts for *Late* (biological replicate 4) infection *vs. Stock* infection.

File S13. Transcript expression and statistical contrasts for *Late* (biological replicate 5) infection *vs. Stock* infection.

File S14. R Script for the figures and statistical analyses.

File S15. Dataset for Figure 2.

File S16. Dataset for Table 1.

File S17. Dataset for Figure 3a.

File S18. Dataset for Figure 3d.

File S19. Dataset for Figure 4.

File S20. Dataset for Figure S3.

File S1. Supplementary information document

for " *The transcriptome of the mosquito host Anopheles gambiae upon infection by different selected lines of the microsporidian parasite Vavraia culicis*" by Luis M. Silva

In this file:

Table S1. Number of genes detected per sample.

Figure S1. Host RNA-sequencing and parasite gene counts.

Figure S2. Quality control clustering and PCAs.

Figure S3. Heatmap of the log-fold change for all transcripts across all biological replicates.

Table S1. Number of genes detected per sample. The number of known *Anopheles gambiae* genes per biological replicate (parasite line) and technical replicate (the number of times the biological replicate was measured) is listed below. Each biological sample (or selection replicate) comprises four technical replicates.

Treatment	Biological replicate	Technical replicate	Sample name	Number of known genes detected
Uninfected	-	1	U11	9303
	-	2	U12	9304
	-	3	U13	9146
	-	4	U14	9328
Infected with **reference parasite (unselected)**	-	1	R11	8973
	-	2	R12	8547
	-	3	R13	8600
	-	4	R14	8801
Infected with parasites selected for **early-transmission**	1	1	E11	9433
	1	2	E12	9043
	1	3	E13	8859
	1	4	E14	8847
	2	1	E21	9113
	2	2	E22	8557
	2	3	E23	9017
	2	4	E24	9282
	3	1	E31	9122
	3	2	E32	8984
	3	3	E33	9020
	3	4	E34	8901
	4	1	E41	8799
	4	2	E42	8982
	4	3	E43	7962
	4	4	E44	9070
	5	1	E51	8807
	5	2	E52	8951
	5	3	E53	8851
	5	4	E54	8784
Infected with parasites selected for **late-transmission**	1	1	L11	9171
	1	2	L12	9094
	1	3	L13	8958
	1	4	L14	9107
	2	1	L21	9083
	2	2	L22	9356
	2	3	L23	9123
	2	4	L24	8929
	3	1	L31	8922
	3	2	L32	9038
	3	3	L33	9193
	3	4	L34	9161
	4	1	L41	8716
	4	2	L42	8855
	4	3	L43	8462
	4	4	L44	7629
	5	1	L51	9386
	5	2	L52	9638
	5	3	L53	9538
	5	4	L54	9136

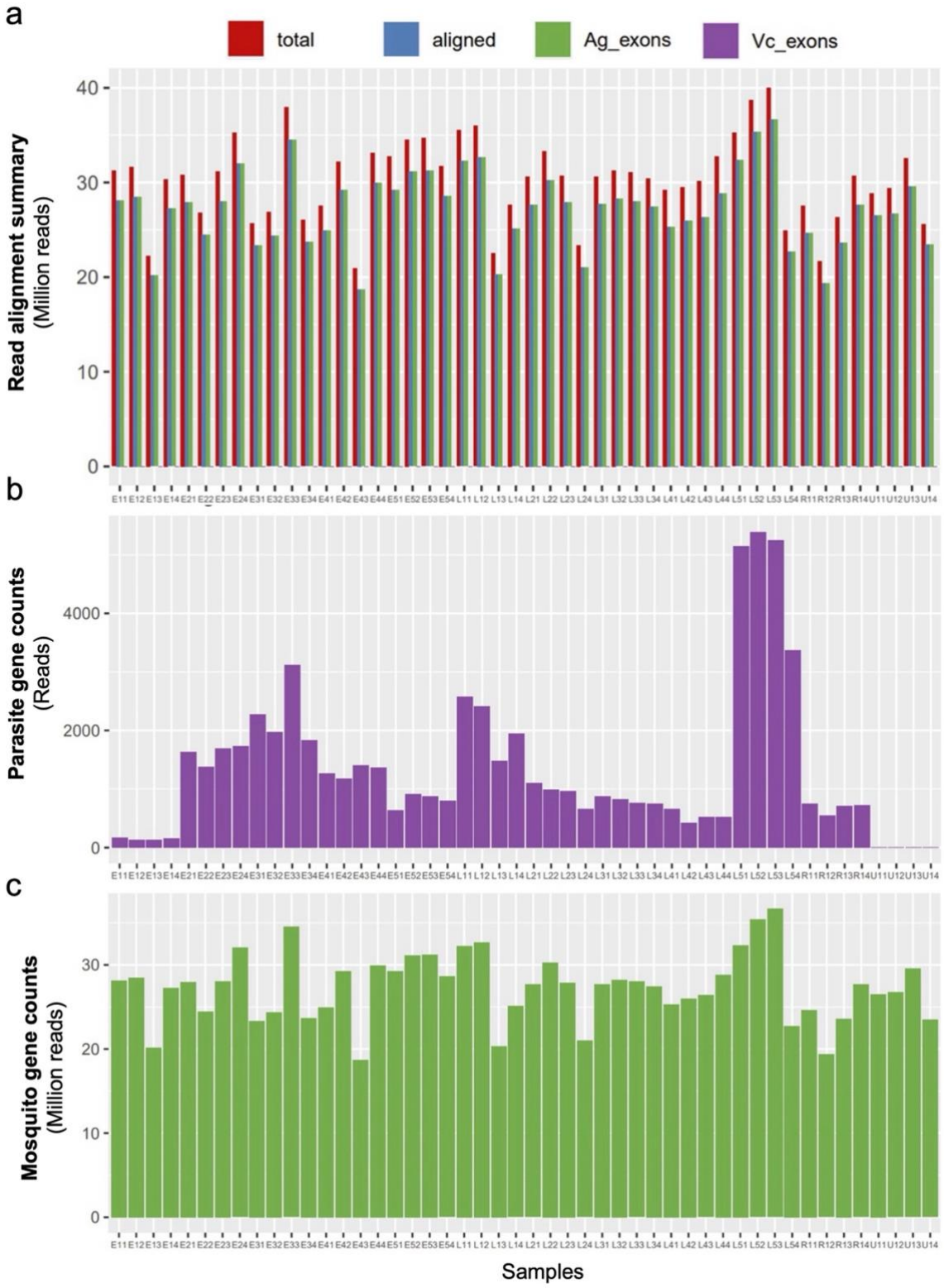

Figure S1. Host RNA-sequencing and parasite gene counts. (a) Barplot showing the number of total reads, the number of aligned reads, and how many of which are *Anopheles gambiae* or *Vavraia culicis* exons. **(b)** Number of V. culicis reads found in each of the biological samples. **(c)** Number of *A. gambiae* reads found in each of the biological replicates and technical replicates.

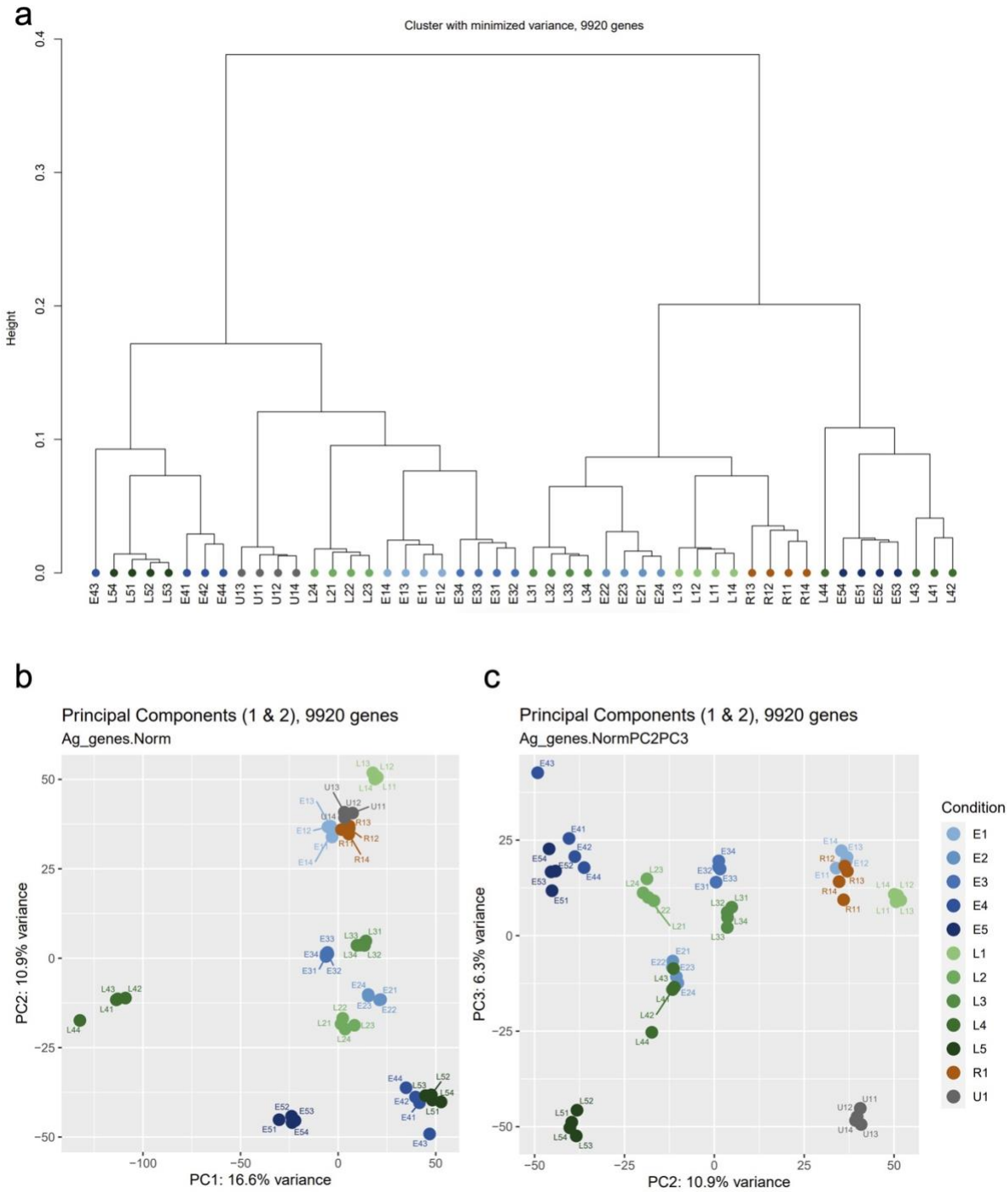

Figure S2. Quality control clustering and PCAs. Statistical quality controls were performed through density gene expression distribution, clustering, and sample PCA. **(a)** Clustering and **(b)** PCA show that replicates group together as expected, with two exceptions for samples E43 and L44. **(c)** Since the first two principal components in the PCA explain only 30% of the variability, a PCA including PC2 and PC3 (an additional 6% of the variability) was considered. The latter does not indicate a clustering of uninfected and unselected reference infections.

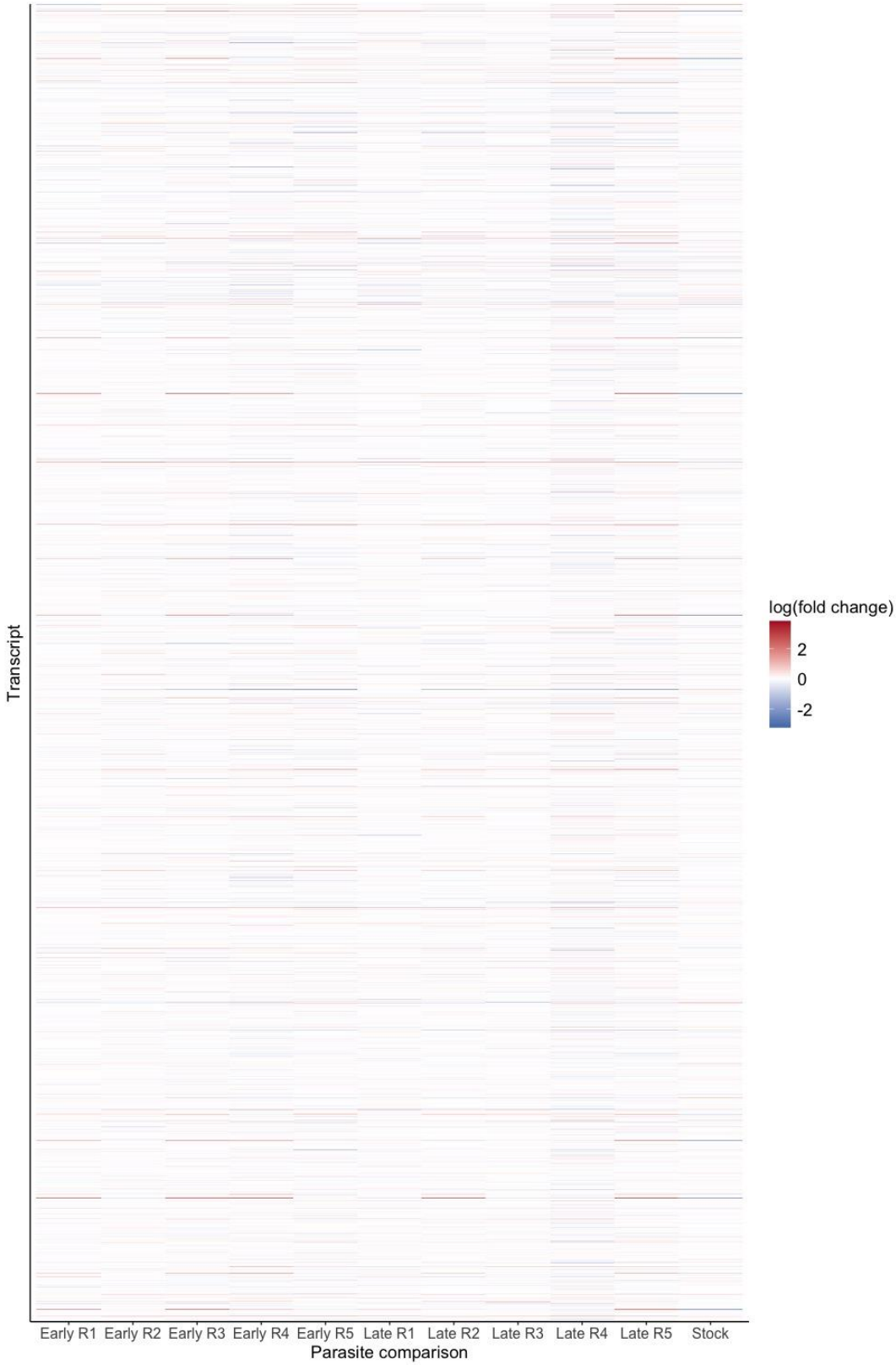

Figure S3. Heatmap of the log-fold change for all transcripts across all biological replicates. Heatmap showing the log-transformed fold-change in the expression of all detected transcripts (i.e., 9920) by parasite treatment comparison. All host samples were compared to the host samples in response to the unselected 'Stock' parasite, except for 'Stock', which was compared to the uninfected host transcriptome.